

# **Optical properties of SiO<sub>2</sub>/TiO<sub>2</sub> thin layers prepared by sol–gel method**

MAREK NOCUN<sup>\*</sup>, SŁAWOMIR KWAŚNY, JOANNA ZONTEK

AGH – University of Science and Technology, Department of Material Science and Ceramic, 30-059 Kraków, al. Mickiewicza 30, Poland,

<sup>\*</sup>Corresponding author: nocun@agh.edu.pl

In this investigation, SiO<sub>2</sub>/TiO<sub>2</sub> thin films were prepared on glass and quartz glass substrates by dip coating sol–gel technique. The films were calcinated at 500 °C for 1 hour. Thickness of the films was estimated by ellipsometric measurements and it was in the range from about 30 nm to 700 nm. Refractive index of the films was also established. Chemical composition of the samples was studied by photoelectron spectroscopy. Transmittances of the samples were characterized using UV–VIS spectrophotometer. Subsequently, band gap energy ( $E_g$ ) was estimated for these films. It was found that band gap energy increases with thickness of the films and their value depends on sodium diffusing from glass substrate.

Keywords: sol–gel, optical properties, band gap energy, SiO<sub>2</sub>–TiO<sub>2</sub> thin films.

## **1. Introduction**

Many kinds of different nanostructured materials have been investigated on their potential applications in photocatalysis, photovoltaic, optical and electro-optical devices for over 20 years [1–3]. TiO<sub>2</sub> is one of the best-known photosensitive and photo-reactive materials [4]. Titanium dioxide thin films have been intensively examined for many optical applications [5]. Since, TiO<sub>2</sub> thin layers show a high reflective index and are transparent in visible light range, they can be used as a dielectric reflecting coating or as a part of antireflecting coating [1]. TiO<sub>2</sub> is often used as a photocatalyst because of its chemical stability, nontoxicity and high quantum yield [2]. Titanium dioxide exists in three different polymorphous phases: rutile, anatase and brookite.

It is known that these phases have got various optical and structural properties [2, 3]. Brookite is one of the orthorhombic structures and both anatase and rutile are tetragonal. Rutile is thermodynamic stable. An optical band gap of rutile is 3.0–3.05 eV [5], and refractive index is about 2.7 [6]. Anatase is one of the low-temperature polymorphs with an optical band gap 3.25 eV and refractive index 2.5. Anatase is thermodynam-

ically unstable and it can be transformed into rutile upon the annealing temperature. The process of post-annealing should be controlled if desirable properties of TiO<sub>2</sub> thin film are required to achieve. It was reported that such a transformation depends on film fabrication technique [5–10]. Although rutile has lower optical band gap it is not effective as a photocatalyst due to high rate of electron–hole recombination. Most desirable phase in the case of photocatalyst is anatase, however, because of higher band gap, it works in UV range.

The main research activity is now focused on improving the efficiency of photocatalyst, especially in the visible region. It can be realized by doping TiO<sub>2</sub> with selected elements [11–13]. As early as 1986 it was reported that photocatalytic activity of TiO<sub>2</sub> can be enhanced by introducing SiO<sub>2</sub> [14].

This article summarizes our study on optical properties of thin films based on SiO<sub>2</sub>–TiO<sub>2</sub> system and showing photocatalytic activity.

## 2. Preparation procedure

### 2.1. Sol preparation

The sol solutions were prepared using tetraethyloorthosilicate (TEOS) and tetraethyloorthotitanate (TEOT), Sigma-Aldrich. Ethanol 95% and 2-propanol (Polish Chemicals) were used as solvents. 1 M HCl (Polish Chemicals) was used to catalyze hydrolysis reaction. Chemical composition of the sols is shown in the Table and preparation procedure in Fig. 1.

T a b l e. Chemical composition of the sols.

| Symbol | TEOS<br>[mol] | C <sub>2</sub> H <sub>5</sub> OH<br>[mol] | TEOT<br>[mol] | H <sub>2</sub> O<br>[mol] | HCl<br>[mol] | C <sub>3</sub> H <sub>8</sub> O<br>[mol] |
|--------|---------------|---|---------------|---------------------------|--------------|--|
| T      | –             | 3   | 0.5           | 1.3                       | 0.025        | 32.75                                    |
| S      | 1             | 3   | –             | 1.3                       | 0.025        | 25.8                                     |
| ST11   | 0.5           | 3   | 0.5           | 1.3                       | 0.025        | 25.8                                     |
| ST21   | 1             | 3   | 0.5           | 1.3                       | 0.025        | 25.8                                     |
| ST12   | 0.5           | 3   | 1             | 1.3                       | 0.025        | 25.8                                     |

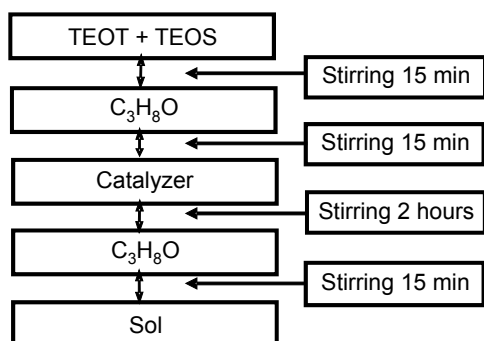


Fig. 1. Sol preparation procedure.

## 2.2. Preparation of thin films

Microscope slide glasses were used as a support. Glasses were first washed in distilled water, dried and washed in ethanol. Both procedures were carried out in ultrasonic bath. Thin films were prepared by dip-coating technique using varying speed of withdrawing. Samples were dried at room temperature and calcinated at  $500\text{ }^\circ\text{C}$  for 30 min. Thicker films were produced by repeating the dipping procedure. The maximum thickness of the film was in the range of 120–800 nm for 1 and 6 coatings, respectively, but varied a little with the kind of sol, and precise value was estimated from ellipsometric measurements – PHE 102 ellipsometer from Angstrom Advance. Cauchy model was applied to evaluate thickness of the sample.

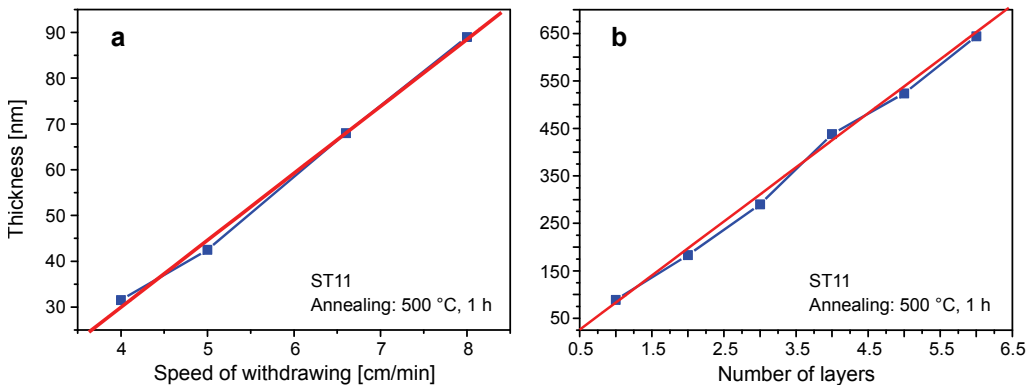


Fig. 2. Thickness of the sample as a function of: withdrawing speed (a), number of layers (b).

Thickness of the sample as a function of withdrawing speed as well as a number of layers is shown in Fig. 2. In the case of one layer sample it was possible to change thickness of the film from about 30 nm to 90 nm by changing the speed of withdrawal. Thicker films were obtained by multilayer deposition. Six layers give film with thickness round 600–650 nm. Each layer was dried at  $150\text{ }^\circ\text{C}$  and baked at  $500\text{ }^\circ\text{C}$  during 1 h before next layer deposition. There was not much difference in the thickness of the film prepared with different sols.

## 2.3. Optical characterization

Optical properties were characterized using UV–VIS spectrophotometer Jasco V-630. Refraction coefficient was measured by spectroscopy ellipsometer PhE-102 Angstrom Advance.

## 2.4. Surface characterization

Surface compositions of the samples were established from XPS measurements using VSW spectrometer. Al  $K\alpha$  200 W was used as an X-ray source. All spectra were calibrated with the binding energy of apparatus carbon C  $1s$  peak  $E_b = 284.6\text{ eV}$  [15–17].

Curve fitting procedure was carried out using XPSPEAK 4.1 program (Raymunda W.M. Kwok, The Chinese University of Hong Kong).

### 3. Results

#### 3.1. Chemical characterization

Chemical composition of the samples was studied by photoelectron spectroscopy. XPS spectra of Ti  $2p$  and Si  $2p$  region for sample ST11 are shown in Fig. 3. Binding energy of titanium Ti  $2p_{3/2}$  was  $458.2 \pm 0.2$  eV, which is a characteristic binding energy of Ti usually observed in the case of  $TiO_2$  [15, 16]. This binding energy was not affected by the amount of titania. Si  $2p$  binding energy of silica in the sample prepared from silica sol – S amounts to 103.1 eV. Binding energy of silica depends on the content of titania in the sample and decreases with increasing amount of Ti. The lowest binding energy of silica 102.0 eV was measured for sample ST12. The lowering in the binding

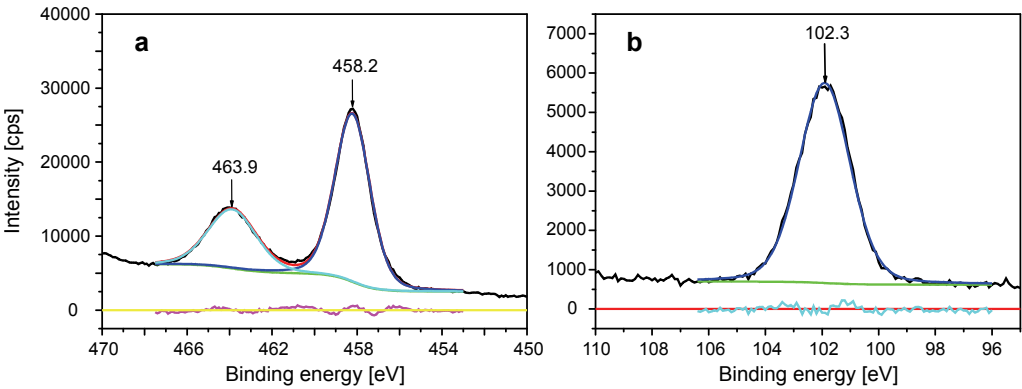


Fig. 3. XPS results of sample ST11. Ti  $2p$  titania region (a), Si  $2p$  silica region (b).

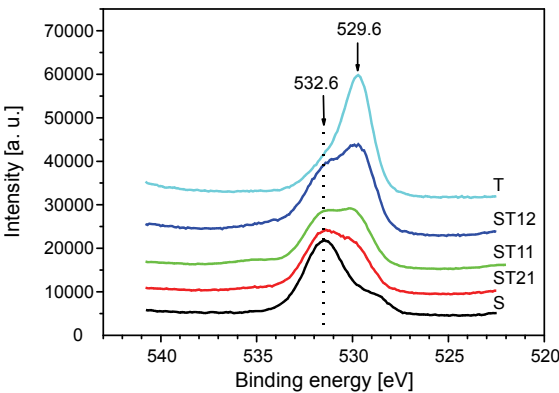


Fig. 4. XPS results for oxygen O  $1s$  region.

energy of Si with Ti content is due to increasing amount of S–O–Ti bridges. This confirms that titanium substitutes some amount of silica and silica-titania network is formed.

Binding energy of oxygen O 1s of the samples under study are shown in Fig. 4. Oxygen connected with titania has binding energy of 529.6 eV. The magnitude of peak with this binding energy is proportional to the amount of titania, see Fig. 4. Oxygen connected with silica has 3 eV higher binding energy: 532.6 eV. Similar value of O(Si) binding energy was reported by MEI *et al.* [18]. Oxygen peak with binding energy 532.6 eV contains also oxygen coming from O–H groups.

### 3.2. Optical properties

All the sols prepared give highly transparent thin films. Transmittance of the samples with two layers (on each side of the glass) deposited at 8 cm/min and fired at 500 °C during 1 h is shown in Fig. 5. The highest transmittance was exhibited by samples prepared from pure  $\text{SiO}_2$  sol – S sample. An increase in  $\text{TiO}_2$  content makes the film more reflective and leads to lower transmittance. The lowest transmittance was observed in the case of T sol, but is still higher than 80%. Transmittance of films prepared on quartz substrate is shown in Fig. 3b. Transmittance of S sample is higher than that of quartz glass because this film has lower refractive index, so it can be applied as antireflection coating. The lowest transmittance was seen for ST12 sample and in the visible range is higher than 80%.

Refractive index of the films was established from ellipsometry measurements. Refractive index is a function of wavelength and for T sample changes from 2.647 at 350 nm to 1.579 at 1000 nm, see Fig. 6. It is much lower than observed in the case of  $\text{TiO}_2$  in polycrystalline powder form:  $n_D = 2.488$  for anatase and indicates high porosity of the layer. Pure  $\text{SiO}_2$  sol gives a layer with low refractive index: from 1.480

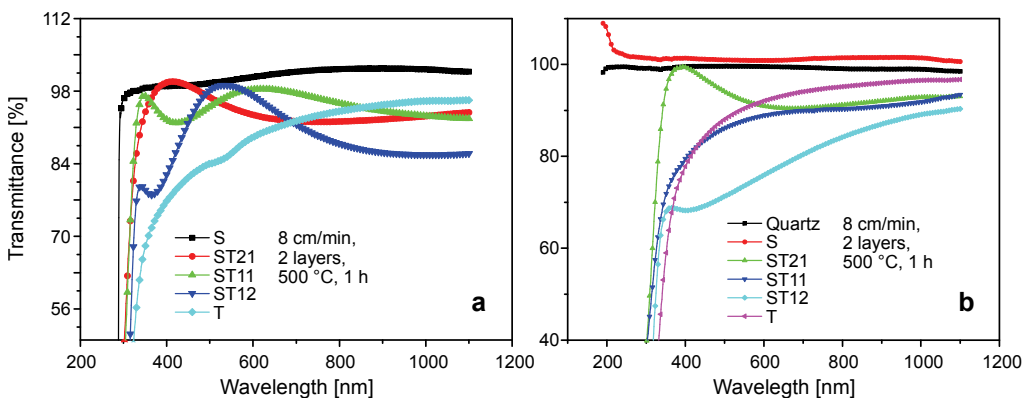


Fig. 5. Transmittance of the samples with two layers of films prepared from the sol indicated in the figure (two layers from each side). Films on soda-lime glass substrate (a), films prepared on quartz glass substrate (b).

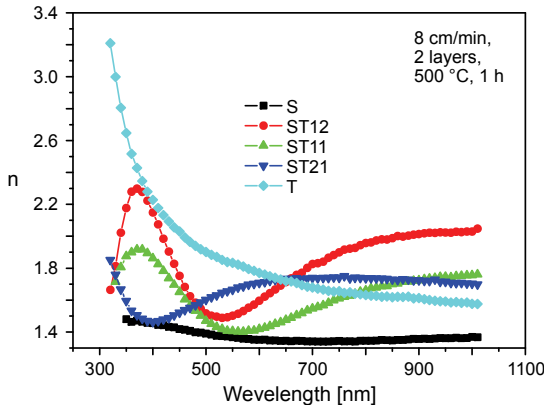


Fig. 6. Refractive index measured for samples annealed at 500 °C during 1 h.

to 1.369 at 350 nm and 1000 nm, respectively. It is also lower than observed for pure SiO<sub>2</sub> glass;  $n_D = 1.458$  while in our case  $n_D = 1.353$ . Refractive index of other samples is changing due to multiple reflection on the film.

Optical band gap of SiO<sub>2</sub>/TiO<sub>2</sub> films deposited on soda-lime glasses is presented in Fig. 7. As the absorption coefficient  $\alpha$  is proportional to  $-\ln(T)$ , where  $T$  is the film transmittance, so to obtain band gap energy,  $[-\ln(T)h\nu]^2$  versus  $h\nu$  was plotted and energy was estimated from interception of straight asymptote line with horizontal axis, see Fig. 7. Sample with lowest concentration of titania – ST21 has the highest value of optical band gap: 4.06 eV, while the lowest value of 3.87 eV was observed for pure titania films –  $T$  sample. The observed value of band gap is much higher than in the case of TiO<sub>2</sub> in crystalline or polycrystalline form and such value is often reported in the case of thin films with nanometer size crystals [19]. We expected also the influence of sodium diffusing from glass on optical band gap of titania. To evaluate

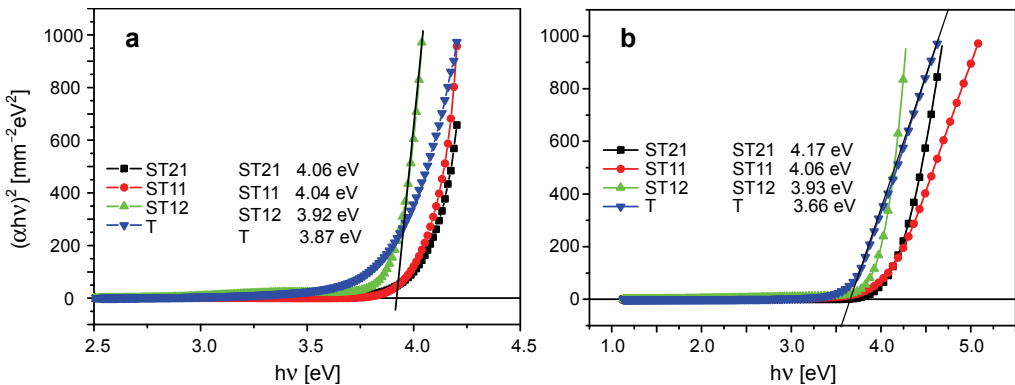


Fig. 7. Optical energy band gap: thin films on soda-lime glass (a), thin films on silica glass (b).

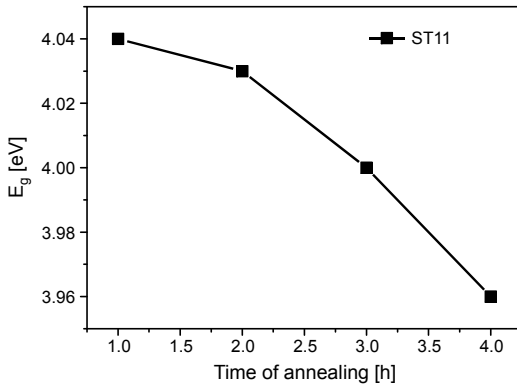


Fig. 8. Influence of annealing time on optical energy band gap.

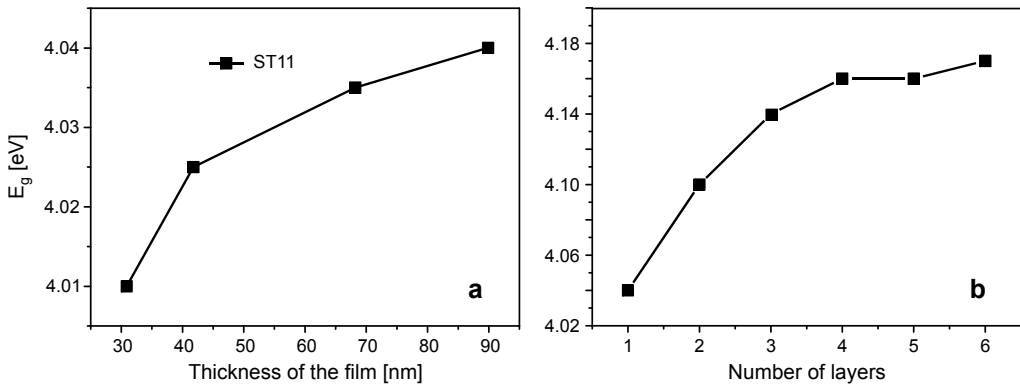


Fig. 9. Optical energy band gap as a function of thickness: one-layer system (a), multilayer system (b).

the influence of sodium on band gap value, we prepared samples on quartz glass substrate. Results are shown in Fig. 7b. Optical band gap was much lower in the case of *T* sample, while in the case of silica-titania films it remains almost unchanged. These changes are most probably due to doping of titania crystals by sodium. Silica-titania films are less sensitive to sodium as in silica matrix crystal growth of TiO<sub>2</sub> is limited [20].

The influence of annealing time on optical energy band gap was studied in the case of ST11 sol deposited on glass, as shown in Fig. 8. Prolongation of annealing time leads to a small decrease of  $E_g$  from 4.04 to 3.96 eV.

The increase in  $E_g$  is due to TiO<sub>2</sub> crystal growth. An increase in thickness of the film leads to an increase in  $E_g$ , but in the case of one layer system this increase is small; from 4.01 to 4.04 eV, see Fig. 9a. In the case of a multilayer system, band gap energy increases up to 4.17 eV – Fig. 9b. The observed increase is due to higher disorder on the boundary of the films.

## 4. Conclusions

Optical films obtained from SiO<sub>2</sub> sol are highly transparent. SiO<sub>2</sub>-TiO<sub>2</sub> sol compositions give reflective films and reflectance is proportional to TiO<sub>2</sub> content. Dip-coating technique allows us to obtain film with thickness from 30 to 90 nm, in the case of one layer coating and thicker films when multilayer technique is applied – up to 700 nm. The measured optical band gap energy decreases with an increase in TiO<sub>2</sub> content and was estimated to be 3.87 eV for pure TiO<sub>2</sub> composition. Lower band gap energy was observed for films prepared on quartz glass than on soda-lime glass. Time of annealing decreases band gap energy. The band gap energy increases with thickness of the film. This effect is especially noticeable in the case of multilayer samples.

## References

- [1] TURNER R.H., BOERIO F.J., *Molecular structure of interfaces formed with plasma-polymerized silica-like primer films: Part III. Mechanical strength and environmental durability of the primer/aluminum and primer/titanium interfaces*, The Journal of Adhesion **78**(6), 2002, pp. 495–504.
- [2] NOGE S., UNO T., SHIMOTORI H., FUJITSUKA S., *Behavior of metal-doped silica thin films with artificial-lattice structure B: Luminescence*, Ferroelectrics **338**(1), 2006, pp. 225–232.
- [3] VAN POPTA A.C., CHENG J., SIT J.C., BRETT M.J., *Birefringence enhancement in annealed TiO<sub>2</sub> thin films*, Journal of Applied Physics **102**, 2007, p. 013517.
- [4] ZHANG X., ZHENG H., *Synthesis of TiO<sub>2</sub>-doped SiO<sub>2</sub> composite films and its applications*, Bulletin of Materials Science **31**(5), 2008, pp. 787–790.
- [5] YAMASHITA H., NISHIO S., IMAOKA S., SHIMADA M., MORI K., TANAKA T., NISHIYAMA N., *Photo-induced surface property on transparent mesoporous silica thin films containing single-site photocatalyst*, Topics in Catalysis **47**(3–4), 2008, pp. 116–121.
- [6] FALARAS P., XAGAS A.P., *Roughness and fractality of nanostructured TiO<sub>2</sub> films prepared via sol-gel technique*, Journal of Material Science **37**(18), 2002, pp. 3855–3860.
- [7] NAGAI H., AOYAMA S., HARA H., MOCHIZUKI CH., TANAKO I., BABA N., SATO M., *Rutile thin film responsive to visible light and with high UV light sensitivity*, Journal of Material Science **44**(3), 2009, pp. 861–868.
- [8] WANG C.M., LIN S.Y., *Electrochromic properties of sputtered TiO<sub>2</sub> thin films*, Journal of Solid State Electrochemistry **10**(4), 2006, pp. 255–259.
- [9] WON D.-J., WANG C.-H., JANG H.-K., CHOI D.-J., *Effects of thermally induced anatase-to-rutile phase transition in MOCVD-grown TiO<sub>2</sub> films on structural and optical properties*, Applied Physics A **73**(5), 2001, pp. 595–600.
- [10] TERJO-VALDEZ M., JENOUVRIER P., FICK J., LANGLET M., *Characterization of optically active and photocurable ORMOSIL thin films deposited using the Aerosol process*, Journal of Material Science **39**(8), 2004, pp. 2801–2810.
- [11] STIR M., NICULA R., BURKEL E., *Pressure-temperature phase diagrams of pure and Ag-doped nanocrystalline TiO<sub>2</sub> photocatalysts*, Journal of the European Ceramic Society **26**(9), 2006, pp. 1547–1553.
- [12] TIAN X.B., WANG Z.M., YANG S.Q., LUO Z.J., FU R.K.Y., CHU P.K., *Antibacterial copper-containing titanium nitride films produced by dual magnetron sputtering*, Surface and Coatings Technology **201**(19–20), 2007, pp. 8606–8609.



- [13] ZHANG H.J., WEN D.Z., *Antibacterial properties of Sb-TiO<sub>2</sub> thin films by RF magnetron co-sputtering*, Surface and Coatings Technology **201**(9–11), 2007, pp. 5720–5723.
- [14] ANPO M., NAKAYA H., KODAMA S., KUBOKAWA Y., DOMEN K., ONISHI T., *Photocatalysis over binary metal oxides. Enhancement of the photocatalytic activity of titanium dioxide in titanium-silicon oxides*, Journal of Chemical Physics **90**, 1986, pp. 1633–1636.
- [15] WAGNER C.D., RIGGS W.M., DAVIS L.E., MOULDER J.F., MUILENBERG G.E., [In] *Handbook of X-Ray Photoelectron Spectroscopy*, Perkin-Elmer, 1976.
- [16] LEI GE, MINGXIA XU, *Fabrication and characterization of TiO<sub>2</sub> photocatalytic thin film prepared from peroxo titanate acid sol*, Journal of Sol-Gel Science and Technology **43**(1), 2007, pp. 1–7.
- [17] BRIGGS D., SEACH M.P., [In] *Practical Surface Analysis*, Wiley and Sons, NY, 1983.
- [18] MEI F., LIU C., ZHANG L., REN F., ZHOU L., ZHAO W.K., FANG Y.L., *Microstructural study of binary TiO<sub>2</sub>:SiO<sub>2</sub> nanocrystalline thin films*, Journal of Crystal Growth **292**(1), 2006, pp. 87–91.
- [19] NURDIWIJAYANTO L., PURWASASMITA B.S., *Optical properties of (100) preferred oriented titanium-doped zinc oxide thin films and their electron trapping phenomena*, Journal of Materials Science and Engineering, November **4**(11), 2010, serial no. 36.
- [20] VISWANATH R.N., RAMASAMY S., *Study of TiO<sub>2</sub> nanocrystallites in TiO<sub>2</sub>-SiO<sub>2</sub> composites*, Colloids and Surfaces A **133**(1–2), 1998, pp. 49–56.

Received January 10, 2011